Mechanism of acoustically induced diffusional structuring of surface adatoms

Chengping Wu, Vladimir Yu. Zaitsev, and Leonid V. Zhigilei

Citation: Appl. Phys. Lett. **103**, 221601 (2013); doi: 10.1063/1.4832996
View online: http://dx.doi.org/10.1063/1.4832996
View Table of Contents: http://apl.aip.org/resource/1/APPLAB/v103/i22
Published by the AIP Publishing LLC.

Mechanism of acoustically induced diffusional structuring of surface adatoms

Chengping Wu,[1] Vladimir Yu. Zaitsev,[1,2] and Leonid V. Zhigilei[1,a)]
[1]Department of Materials Science and Engineering, University of Virginia, Virginia 22904, USA
[2]Institute of Applied Physics, Russian Academy of Sciences, Nizhny Novgorod, Russia

(Received 28 August 2013; accepted 7 November 2013; published online 25 November 2013)

Physical mechanisms of time-averaged structuring of adatoms induced by a standing surface acoustic wave (SAW) on a solid substrate are studied. Despite some similarity with conventional mechanisms based on averaging of fast oscillation-type motion or radiation-pressure effects, we demonstrate that, for diffusional (i.e., strongly damped) adatom motion, the origin of time-averaged structuring is essentially different. The proposed analytical model and kinetic Monte–Carlo (kMC) simulations reveal several distinct structuring regimes and directly relate them to the transient modification of diffusion barriers and adiabatic temperature variations induced by SAW strains. © *2013 AIP Publishing LLC*. [http://dx.doi.org/10.1063/1.4832996]

The phenomenon of average forces acting on particles in oscillating fields has long been attracting interest[1–3] that is renewed now[4] in view of novel lab-on-a-chip applications, e.g., for structuring of particles suspended in liquids and non-contact manipulation of acoustically trapped individual micro-particles.[5–7] A discussion in Ref. 3 of the appearance of time-averaged forces acting on particles subjected to symmetric-in-time but spatially non-uniform oscillating force emphasizes that, in the absence of other forces, an oscillating particle tends to positions where its kinetic energy is minimal. Thus, the kinetic energy of the particle oscillations plays the role of an effective potential. Hereafter, we call this mechanism inertial, since inertia (non-zero particle's mass) is essential for appearance of the average force. A manifestation of this mechanism is gathering of charged particles in nodes of an oscillating electric field regardless of the sign of the charge.[8,9] In the presence of other potential forces, new equilibrium positions can appear for the total effective potential. This is exemplified by a well-known case of a rigid pendulum with the oscillating suspension point, for which counter-intuitive local equilibrium at the upper point may appear.[3]

Another commonly discussed mechanism of average-force appearance is the radiation mechanism.[1,2,4] Unlike the inertial one, it can operate even for spatially uniform, on average, running fields. Scattering of the incident wave by a particle causes the mechanical momentum transfer and results in the appearance of time-averaged force. Under certain conditions, the radiation force may act along with the inertial one. For example, particles in liquids subjected to acoustic waves can experience both the inertial force (due to the difference in densities of the liquid and particles) and the radiation force (due to the difference in the compressibility, even if the densities are equal). This interplay determines the so-called Gorkov's acoustic radiation-force potential for particles in liquids[10] and its extensions accounting for viscosity.[4,11]

Recently, intriguing results of molecular dynamics (MD) simulations were reported for even smaller objects: nanostructuring of adatoms was induced by a standing surface acoustic wave (SAW) on a solid substrate.[12] Since for individual atoms radiation pressure due to acoustic wave re-radiation is irrelevant, the physical origin of the computational results[12] was discussed in Refs. 12–14 within the framework of the attractively clear inertial mechanism[3] which, in principle, is applicable to individual ions and electrons (e.g., in plasmas).[8,9] However, despite the apparent qualitative similarity between the results of the theoretical analysis[13,14] and MD simulations,[12] the questions on the dependence of the characteristics of nanostructuring on the parameters of SAW and, more generally, on applicability of the inertial mechanism to realistic material systems remain open.

In this Letter, we report an approximate analytical model and results of kinetic Monte-Carlo (kMC) simulations which reveal a specific, essentially diffusional, mechanism of acoustically induced time-averaged structuring of surface adatoms. This mechanism has not been discussed earlier and cannot be reduced to conventional paradigms of inertia- and radiation-induced average forces. We found an explicit relationship between the acoustic strains and their average action, which revealed a rich variety of possible structuring regimes.

Before turning to the discussion of the diffusional mechanism, we show that the conventional inertial mechanism of the averaged drift of adatoms in response to an oscillating force is inoperable due to the strong damping (effective viscosity) intrinsic to the diffusional motion. To evaluate the roles of damping and inertia for the time-averaged motion of a particle of mass m oscillating in the presence of damping with effective coefficient α, we consider a representative case of a sinusoidal standing wave force field with amplitude F_0, angular frequency Ω, and wavenumber k, described by the following equation:

$$m\ddot{x} + \alpha\dot{x} = F_0 \cos(\Omega t)\sin(kx). \quad (1)$$

To obtain the time-averaged motion, the solution can be represented as a sum $x(t) = X(t) + \zeta(t)$ of the slowly varying term $X(t)$ and rapidly oscillating term $\zeta(t)$. Conventional procedures[3,12] yield the following solution for $\zeta(t)$ in the first-order of F_0:

a)Author to whom correspondence should be addressed. Electronic mail: lz2n@virginia.edu.

$$\zeta(t) = -\frac{F_0 \sin(kX)m}{\alpha^2 + m^2\Omega^2}\cos(\Omega t) + \alpha\frac{F_0 \sin(kX)}{\alpha^2 + m^2\Omega^2}\frac{\sin(\Omega t)}{\Omega}. \quad (2)$$

For small-amplitude oscillations $\zeta k \ll 1$, the slow part of the particle motion, $X(t)$, obeys the equation similar to Eq. (1) with a time-averaged force in its right-hand side (rhs)

$$m\ddot{X} + \alpha\dot{X} \approx \langle k\zeta(t)F_0\cos(\Omega t)\cos[kX(t)]\rangle \equiv -\partial W_{eff}/\partial X, \quad (3)$$

where the effective potential W_{eff} for the slow motion is

$$W_{eff} = \frac{1}{4}\frac{mF_0{}^2}{\alpha^2 + m^2\Omega^2}\sin^2(kX). \quad (4)$$

Notice that, since $\langle\cos(\Omega t)\sin(\Omega t)\rangle = 0$, the second term in Eq. (2) (that is in quadrature with the force) does not contribute to W_{eff}. This means that increasing α shifts $\zeta(t)$ out of phase with the force and eliminates the effective potential for $\alpha \gg \Omega m$. In energy terms, this means that the role of kinetic energy of the primary oscillatory motion of the particle becomes negligible (inertia is small compared with viscous forces). For given Ω and m, Eq. (4) indicates that the damping coefficient should be sufficiently small, i.e., $\alpha/m \ll \Omega$, for the inertial effects to become prominent (alternatively, for a fixed α, the dominance of inertia means $\Omega \gg \Omega^* = \alpha/m$).

To evaluate the role of inertia, one needs to estimate the effective damping coefficient α for diffusing adatoms. To this end, one may turn to the classical Langevin equation, $m\ddot{x} + \alpha\dot{x} = f(t)$, describing diffusional motion of a particle under the action of a random force $f(t)$ mimicking the thermal fluctuations. The effective damping coefficient α in Eq. (1) has the same physical meaning as in the Langevin equation, for which the value of α can be related to the diffusion coefficient D at temperature T through the Einstein–Smoluchowski relation:[15] $\alpha = k_BT/D$, where k_B is the Boltzmann constant.

Even for an active diffusion with $D \sim 10^{-10}$–10^{-9} m^2/s, temperature of hundreds of K, and adatom mass of ~100 amu, the condition for efficiency of the inertial mechanism is $\Omega \gg \Omega^* = \alpha/m \sim 10^{14}$–$10^{15}$ s^{-1}. Such a frequency of the acoustic wave required for the dominance of the inertial effects is several orders of magnitude higher than the frequency of atomic vibrations (the Debye frequency is $\Omega_D \sim 10^{13}$s$^{-1} < \Omega^*$). This suggests that for any SAW with a realistic frequency, the inertial mechanism of generation of time-averaged forces is completely suppressed for the diffusional motion of surface adatoms.

Since the commonly discussed inertial and radiation-force mechanisms are not relevant to the acoustically induced structuring of surface adatoms, we now focus on revealing an alternative mechanism that is consistent with diffusional nature of adatoms mobility. As a starting point, we note that the acoustic strain $e(x,t)$ can modify the instantaneous values of both the diffusion barrier E_d and surface temperature T, thus affecting the adatom jump rate determined by the Arrhenius law

$$r(x,t) = R_0\exp\left(-\frac{E_d[e(x,t)]}{k_BT[e(x,t)]}\right), \quad (5)$$

where R_0 is the so-called attempt frequency related to the vibrational frequency of a surface adatom. The two conditions for applicability of the Arrhenius law to the description of surface diffusion in the presence of SAWs are: (i) the absence of the direct dynamic coupling of SAW to the adatom vibrations and (ii) the time of equilibration of the adatom with the substrate being much shorter than the period of SAW.[22] These conditions are readily satisfied for conventional sources of SAWs.

The effect of strain on the energy landscape for adatom diffusion is schematically illustrated in Fig. 1. The results of quasi-static *ab initio*[16–19] and classical[20] atomistic calculations suggest that, for a broad range of material systems, the variation of the binding energy E_B and the saddle point energy E_S of an adatom on a strained surface can be fairly well approximated by linear dependences up to surface strains of several percent, i.e., $E_B(e) \approx E_B^0 + \beta_B e$ and $E_S(e) \approx E_S^0 + \beta_S e$, where E_B^0 and E_S^0 are the binding and saddle point energies in the absence of strain. The strain dependence of the corresponding diffusion barrier, $E_d = E_S - E_B$, can be described as

$$E_d(e) \approx E_d^0 + \gamma e, \quad (6)$$

where E_d^0 is the diffusion barrier at a strain-free surface and $\gamma = \beta_S - \beta_B$.

For inhomogeneous uniaxial strain $e = e(x,t)$, such as the one generated by SAWs, the modification of the surface energy landscape is not limited to the variation of the local diffusion barrier given by Eq. (6) but also includes the asymmetry of the diffusion barriers for adatom jumps along and counter the strain gradient, i.e., $E_{d,p}(x)$ and $E_{d,q}(x)$ for jumps in the left and right directions in Fig. 1 are not equal to each other and

$$E_{d,q}(x) - E_{d,p}(x) \approx \delta \cdot b \cdot \partial e/\partial x. \quad (7)$$

Here, b is the adatom jump distance in x direction, δ is the diffusion barrier asymmetry parameter that can readily be shown to be equal to β_S, and the average diffusion barrier in Eq. (6) is $E_d(e) = (E_{d,p} + E_{d,q})/2$. As demonstrated below,

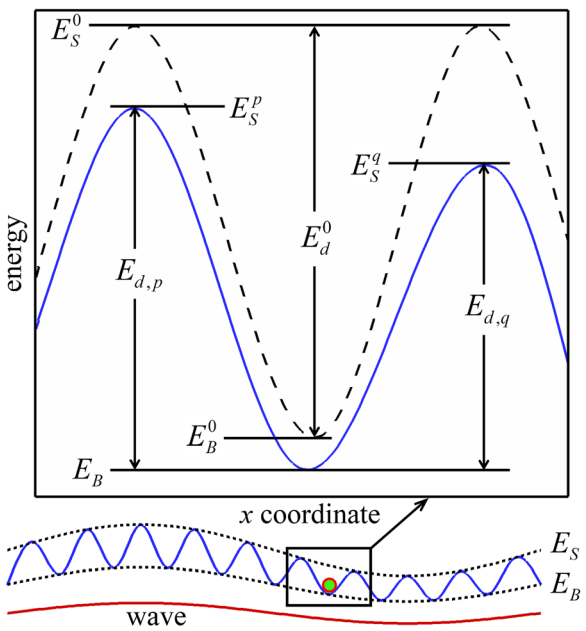

FIG. 1. Schematic illustration of the effect of surface strain generated by a SAW on the energy landscape for adatom diffusion. The dashed and solid lines in the upper plot show the energy barriers for adatom diffusion without and with the SAW, respectively.

it is the interplay of the diffusion barrier inhomogeneity [Eq. (6)] and asymmetry [Eq. (7)] that largely defines the characteristics of the acoustically induced structuring of surface adatoms.

Besides the modification of the surface energy landscape, the adatom jump rate given by Eq. (5) can be affected by transient changes of surface temperature associated with the variation of the acoustic strain. The reversible adiabatic heating and cooling[21] occur even if the substrate acts as an efficient thermostat and trivial heating due to the wave dissipation is negligible. The nearly adiabatic variations in T are approximately linear in strain and can be expressed as

$$T(e) \approx T_0 - T_0\theta e(x,t), \tag{8}$$

where T_0 is the temperature of the substrate and the parameter θ is defined by the elastic moduli, heat capacity, and coefficient of thermal expansion of the substrate material.[21] For small changes of the surface temperature ($\Delta T \ll T_0$), the effect of the adiabatic temperature variation on the adatom jump rate given by Eq. (5) can be approximated by an equivalent variation in the diffusion barrier, $E_d^T(e) \approx E_d^0 + \gamma_T e$, where $\gamma_T = \theta E_d^0$.[22] By introducing $\gamma_{eff} = \gamma + \gamma_T$, the combined effect of the adiabatic temperature variation and the modification of the diffusion barriers given by Eq. (6) can then be described in terms of an effective variation in the diffusion barrier

$$E_d^{eff}(e) \approx E_d^0 + \gamma_{eff} e. \tag{9}$$

Now, with the understanding of the strain effect on key parameters controlling diffusion, the time-averaged structuring of adatoms in the presence of a standing SAW can be considered by solving 1D kinetic equation

$$\partial n(x)/\partial t = \nu_+ - \nu_-, \tag{10}$$

where $n(x)$ is the adatom density at a site located at x, $\nu_-(x) = n(x)[r_p(x) + r_q(x)]$ and $\nu_+(x) = n(x+b)r_p(x+b) + n(x-b)r_q(x-b)$ are the rates of adatom jumps from/to neighboring sites with coordinates $x \pm b$, r_p and r_q are the jump rates to the left and to the right defined by the Arrhenius law with corresponding barriers $E_{d,p}$ and $E_{d,q}$ that are perturbed by acoustic strain $e(x,t)$. In what follows, by analogy with the rhs of Eq. (1), we consider an oscillating strain field that corresponds to a standing SAW, $e(x,t) = e_0 \cos(\Omega t)\sin(kx)$.

We denote the uniform unperturbed density as n_0 and its dimensionless perturbation as $N = (n - n_0)/n_0$. Then, recalling that for acoustic waves $kb \ll 1$, combining Eq. (10) with Eqs. (5), (7), and (9), and expanding the exponent in Eq. (5) to the quadratic in e_0 and kb perturbations in E_d^{eff}, one obtains the following diffusion equation for N:

$$\frac{\partial N}{\partial t} - r_0 b^2 \frac{\partial^2 N}{\partial x^2} \approx b^2 \frac{\partial^2}{\partial x^2}[R(x,t) + R(x,t)N] + b\frac{\partial}{\partial x}[Q(x,t) + Q(x,t)N], \tag{11}$$

where r_0 is the unperturbed jump rate given by Eq. (5) at $e = 0$, and the acoustically induced "force" in the right-hand side is defined by $R(x,t) = (r_p + r_q)/2 - r_0$ and $Q(x,t) = r_p - r_q$ that characterize the variations in the adatom jump rates due to the acoustically induced modification of the magnitudes of the effective diffusion barriers [Eq. (9)] and their left-right asymmetry [Eq. (7)], respectively. If the exponent in Eq. (5) is expanded to the second order in strain, $R(x,t)$ and $Q(x,t)$ can be approximated as

$$R \approx R^{(1)} + R^{(2)} = -\frac{r_0\gamma_{eff}e}{k_BT_0} + \frac{r_0}{2}\left(\frac{\gamma_{eff}e}{k_BT_0}\right)^2, \tag{12}$$

$$Q \approx Q^{(1)} + Q^{(2)} = \frac{r_0 b\delta\partial e/\partial x}{k_BT_0} - \frac{r_0 b\delta\gamma_{eff} e\partial e/\partial x}{(k_BT_0)^2}. \tag{13}$$

The "force" in the rhs of Eq. (11) comprises two terms that do not depend on N and are directly determined by the strain-dependent perturbation of the Arrhenius jump rates described by the quantities R and Q, which are approximated by Eqs. (12) and (13). The other two terms contain products RN and QN and are due to the fact that the rates $\nu_\pm$ in the kinetic Eq. (10) are proportional to the local density of the adatoms and the probabilities of leaving or entering a given atomic site.

For an oscillating acoustic strain field, the linear-in-strain components $R^{(1)}$ and $Q^{(1)}$ entering the rhs of Eq. (11) yield the linear-in-strain oscillating perturbation $N^{(1)}$ of the adatom density. Then, in the next approximation, quadratic-in-strain terms $R^{(1)}N^{(1)}$ and $Q^{(1)}N^{(1)}$ in Eq. (11) lead to the time-averaged (over a SAW period) perturbation of adatoms' concentration. This "cascade" mechanism, however, is extremely damped for any realistic SAW parameters and, for a given k, it can be activated only for $\Omega \to 0$, i.e., for *static* periodic strain $e(x) = e_0 \sin(kx)$ rather than oscillating acoustic strain. While this mechanism may control nucleation of self-assembled islands on surfaces where static periodic strain field is created by dislocation arrays[23] or buried strained islands,[24,25] it does not contribute to the acoustic structuring and is not considered further in the present paper.

The quadratic-in-strain terms ($R^{(2)}$ and $Q^{(2)}$) entering the rhs of Eq. (11) due to nonlinearity of the Arrhenius rate equation, on the other hand, directly yield non-zero perturbation in the adatoms' concentration averaged over the SAW period, $\bar{N}$. The leading term that provides an estimate for the time-scale and magnitude of structuring induced by the acoustic strain has the following form:

$$\bar{N}(x,t) \approx [1 - \exp(-t/\tau)]\frac{\gamma_{eff}(\gamma_{eff} - \delta)}{8(k_BT_0)^2} e_0^2 \cos(2kx), \tag{14}$$

where the characteristic structuring time $\tau = 1/(4b^2k^2r_0)$.

Several conclusions can be derived from the approximate scaling law given by Eq. (14) for the acoustic structuring.

First, similar to the inertial mechanism described by Eq. (1), the spatial period of the diffusional structuring is twice smaller than the wavelength of SAW, $\lambda = 2\pi/k$. This similarity prevents the discrimination of the mechanisms by the period of structuring and is due to the trivial reason that both effects in the lowest approximations are quadratic in strain.

Second, the wavelength of SAW does not affect the ultimate structuring contrast $\bar{N}(x, t \to \infty)$ but defines the characteristic structuring time τ. This is an important conclusion

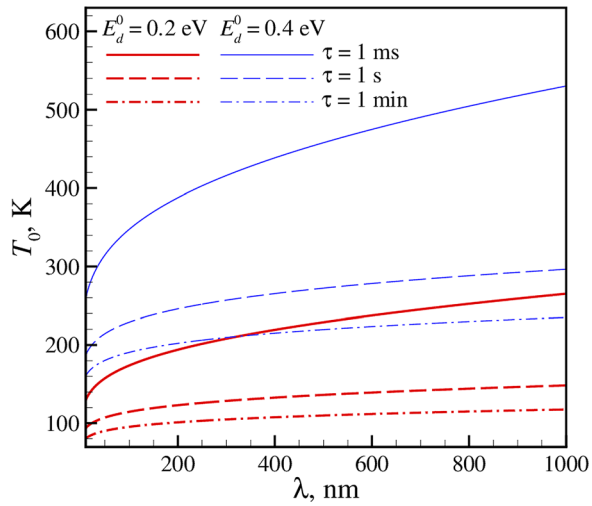

FIG. 2. Isochrone curves of the structuring time τ as functions of the substrate temperature T_0 and SAW wavelength $\lambda = 2\pi/k$ for representative values of $b = 0.2$ nm, $R_0 = 1$ ps^{-1}, and E_d^0 equal to 0.2, and 0.4 eV, as predicted by the analytical model, Eq. (14). The solid, dashed, and dash-dotted curves are for τ equal to 1 ms, 1 s, and 1 min, respectively.

indicating that the effect of surface structuring is not limited to extreme frequencies of hundreds of GHz[12] and can be achieved with conventional sources of SAWs. As illustrated in Fig. 2, the quadratic increase of the structuring time with wavelength, $\tau \sim \lambda^2$, characteristic of the diffusional redistribution of the adatoms, can be counteracted by a moderate temperature increase that affects the structuring time through the strong Arrhenius temperature dependence of r_0 given by Eq. (5) with $e = 0$. The increase in T_0 reduces the ultimate structuring contrast [see Eq. (14)] and the optimal choice of T_0 is defined by the balance between the sufficiently high level of structuring contrast and reasonably short structuring time. Since the temperature T_0 that yields the value of r_0 needed to ensure a reasonable time of structuring for given parameters of the SAW is determined by the magnitude of E_d^0, the material parameter that controls the structuring is $\gamma_{eff}(\gamma_{eff} - \delta)/(E_d^0)^2$.

Finally, the factor $\gamma_{eff}(\gamma_{eff} - \delta)$ in Eq. (14) suggests that an interplay between strain-induced variations of surface temperature [Eq. (8)] and magnitude of diffusion barriers [Eq. (6)], as well as local asymmetry of the barriers associated with the gradient of the acoustic strain [Eq. (7)] results in the existence of several distinct regimes of surface structuring, namely:

(i) gathering of adatoms in the regions of SAW-strain nodes when ($\gamma_{eff} > 0$ and $\gamma_{eff} > \delta$) or ($\gamma_{eff} < 0$ and $\gamma_{eff} < \delta$), e.g., Fig. 3(a);
(ii) gathering of adatoms in the regions of SAW-strain antinodes when ($\gamma_{eff} < 0$ and $\gamma_{eff} > \delta$) or ($\gamma_{eff} > 0$ and $\gamma_{eff} < \delta$), e.g., Fig. 3(b);
(iii) absence of structuring when the effective barrier-height variation is either absent ($\gamma_{eff} = 0$) or is compensated by the barrier asymmetry ($\gamma_{eff} = \delta \neq 0$).

The accuracy of the approximations used in the derivation of Eq. (14) can readily be evaluated in one-dimensional kMC simulations of surface diffusion[22] in the presence of a standing SAW. The simulations directly implement the discrete kinetic Eq. (10) in which the jump rates to the left and right, r_p and r_q, are defined by the Arrhenius law with corresponding diffusion barriers, $E_{d,p}$ and $E_{d,q}$ [Eqs. (6) and (7)], and instantaneous temperature given by Eq. (8). The results of kMC simulations performed for two distinct regimes of surface structuring are shown in Fig. 3 along with the theoretical predictions. Both the time evolution of the density profiles and the final structuring contrasts predicted in the simulations are well described by the theoretical curves. Minor discrepancy between the approximate analytical and kMC results is mainly related to the quadratic-in-strain expansion of the Arrhenius equation that becomes less accurate at lower temperatures.

The feasibility of different structuring regimes in real material systems can be evaluated by considering the results of atomistic simulations of adatom diffusion on strained surfaces. In particular, recent simulations of adatom diffusion on a uniaxially strained (001) surface of a Lennard–Jones (LJ) crystal[22] reveal non-monotonous variations of γ/E_d^0 between 1.1 to 2.6 and δ/E_d^0 between 0.5 to 12.0 as the size of the adatom changes from 0.8 to 1.5 of the size of atoms in the substrate. With $\gamma_T/E_d^0 = 1.5$ evaluated for the LJ substrate, these variations correspond to values of $\gamma_{eff}(\gamma_{eff} - \delta)/(E_d^0)^2$ ranging from -33.5 to 7.0 (Fig. 3 illustrates these two limiting cases). Even larger values of $\gamma(\gamma - \delta)/(E_d^0)^2$ can be obtained based on the results of *ab initio* calculations performed for biaxially strained substrates, e.g., 539 for Ge/Ge(001),[19] -3 for Ge/Si(001),[19] -14 for In/GaAs(001),[18] and 299 for Ag/Ag(111).[16]

The broad variability of the parameters that control surface structuring in different material systems indicates that different structuring regimes (gathering of adatoms in SAW-strain nodes or antinodes) may be realized for different substrate - adsorbate combinations. For an adsorbate that makes one successful jump per 10^4 "attempts" (jump rate of $\sim$1–10 ns^{-1}), i.e., $k_B T_0 = E_d^0/(4 \ln 10)$, the structuring contrast, $\sim[\gamma_{eff}(\gamma_{eff} - \delta)/(E_d^0)^2] \times 10 e_0^2$, can be sufficiently

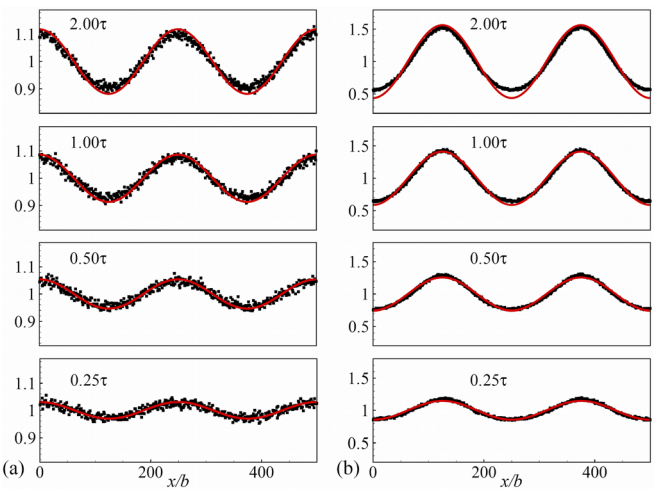

FIG. 3. Examples of SAW-induced gathering of adatoms in the regions of SAW-strain nodes (a) and anti-nodes (b). Density profiles are shown for different times given in units of characteristic structuring time τ. Red solid curves show predictions of Eq. (14) and black symbols are the results of kMC simulations. (a) is for a system with $\gamma = 0.91$ eV, $\delta = 0.30$ eV, $\theta = 1.5$, $E_d^0 = 0.66$ eV, $k_B T_0/E_d^0 = 0.1$ ($T_0 = 770$ K), i.e., $\gamma_{eff}(\gamma_{eff} - \delta)/(E_d^0)^2 = 7.0$ and (b) is for a system with $\gamma = 0.43$ eV, $\delta = 1.95$ eV, $\theta = 1.5$, $E_d^0 = 0.16$ eV, $k_B T_0/E_d^0 = 0.1$ ($T_0 = 190$ K), i.e., $\gamma_{eff}(\gamma_{eff} - \delta)/(E_d^0)^2 = -33.5$. The same strain magnitude $e_0 = 0.04$ is used in both simulations.

strong to induce acoustically guided nucleation of 2D islands of adatoms.

Even stronger structuring can be achieved with SAWs of extremely high frequencies on the order of 100s of GHz, when the direct dynamic coupling between the acoustic wave and surface vibrations of adsorbates is possible. The results of recent MD simulations demonstrate that the dynamic (near-resonance) coupling is capable of strongly enhancing surface diffusion for running SAWs[22] and surface structuring for standing SAWs.[12] While the prospects for practical realization of the regime of dynamic coupling are boosted by recent advances in the development of photoacoustic methods for generation of SAWs with frequencies approaching and exceeding 100 GHz,[26–28] strong attenuation and dispersion of high-frequency SAWs may limit utilization of this regime in applications. In contrast, the non-resonant diffusional structuring regimes discussed in the present work have a relatively weak sensitivity to λ (Fig. 2) and may be explored with conventional sources of SAWs.

In summary, theoretical analysis of the phenomenon of structuring of surface adatoms in the presence of standing SAWs reveals a distinct diffusional mechanism that cannot be reduced to conventional paradigms based on analysis of inertial (i.e., related to minimization of kinetic energy of the particle oscillations)[3,8,9] and radiation-induced[1,2,4] average forces produced by oscillating inhomogeneous fields. The diffusional redistribution of surface adatoms is defined by a complex interplay between acoustically induced transient modification of the diffusion barriers, local barrier asymmetry, and adiabatic temperature variations. Explicit relationships between the SAW parameters and the effective "forces" controlling the characteristic time of diffusional structuring and its ultimate contrast are derived analytically and verified in kMC simulations. A rich variety of structuring regimes, which are difficult to foresee intuitively, is established and related to the parameters of SAW and substrate-adatom interactions. Mapping the theoretical predictions to real material systems indicates that practical realization of surface structuring is feasible and suggests an attractive route for acoustic control of surface self-assembly without permanent modification of the substrate and growth conditions.

The financial support from DARPA and computational support from NSF/XSEDE (TG-DMR110090) and OLCF (MAT048) are gratefully acknowledged.

[1]L. V. King, "On the acoustic radiation pressure on spheres," Proc. R. Soc. London, Ser. A **147**, 212–240 (1934).
[2]K. Yosioka and Y. Kawasima, "Acoustic radiation pressure on a compressible sphere," Acustica **5**, 167–173 (1955).
[3]L. D. Landau and E. M. Lifshitz, *Mechanics* (Pergamon Press, Oxford, 1960).
[4]M. Settnes and H. Bruus, "Forces acting on a small particle in an acoustical field in a viscous fluid," Phys. Rev. E **85**, 016327 (2012).
[5]C. D. Wood, S. D. Evans, J. E. Cunningham, R. O'Rorke, C. Wälti, and A. G. Davies, "Alignment of particles in microfluidic systems using standing surface acoustic waves," Appl. Phys. Lett. **92**, 044104 (2008).
[6]J. Shi, D. Ahmed, X. Mao, S. -C. S. Lin, A. Lawit, and T. J. Huang, "Acoustic tweezers: Patterning cells and microparticles using standing surface acoustic waves (SSAW)," Lab Chip **9**, 2890–2895 (2009).
[7]Z. Wang and J. Zhe, "Recent advances in particle and droplet manipulation for lab-on-a-chip devices based on surface acoustic waves," Lab Chip **11**, 1280–1285 (2011).
[8]A. V. Gaponov and M. A. Miller, "Potential wells for charged particles in a high-frequency electromagnetic field," Zh. Eksp. Teor. Fiz. **34**, 242–243 (1958); [Sov. Phys. JETP **7**, 168–169 (1958)].
[9]B. M. Bolotovskii and A. V. Serov, "Details of the motion of charged nonrelativistic particles in a variable field," Phys. Usp. **37**, 515–516 (1994).
[10]L. P. Gor'kov, "On the forces acting on a small particle in an acoustical field in an ideal fluid," Sov. Phys. Dokl. **6**, 773–775 (1962).
[11]A. A. Doinikov, "Acoustic radiation pressure on a compressible sphere in a viscous fluid," J. Fluid Mech. **267**, 1–22 (1994).
[12]C. Taillan, N. Combe, and J. Morillo, "Nanoscale self-organization using standing surface acoustic waves," Phys. Rev. Lett. **106**, 076102 (2011).
[13]N. Combe, C. Taillan, and J. Morillo, "Unidimensional model of adatom diffusion on a substrate submitted to a standing acoustic wave. I. Derivation of the adatom motion equation," Phys. Rev. B **85**, 155420 (2012).
[14]C. Taillan, N. Combe, and J. Morillo, "Unidimensional model of adatom diffusion on a substrate submitted to a standing acoustic wave. II. Solutions of the adatom motion equation," Phys. Rev. B **85**, 155421 (2012).
[15]W. T. Coffey, Y. P. Kalmykov, and J. T. Waldron, *The Langevin Equation with Applications in Physics, Chemistry and Electrical Engineering*, 2nd ed. (World Scientific, Singapore, 2003).
[16]C. Ratsch, A. P. Seitsonen, and M. Scheffler, "Strain dependence of surface diffusion: Ag on Ag(111) and Pt(111)," Phys. Rev. B **55**, 6750–6753 (1997).
[17]D. J. Shu, F. Liu, and X. G. Gong, "Simple generic method for predicting the effect of strain on surface diffusion," Phys. Rev. B **64**, 245410 (2001).
[18]E. Penev, P. Kratzer, and M. Scheffler, "Effect of strain on surface diffusion in semiconductor heteroepitaxy," Phys. Rev. B **64**, 085401 (2001).
[19]A. van de Walle, M. Asta, and P. W. Voorhees, "First-principles calculation of the effect of strain on the diffusion of Ge adatoms on Si and Ge(001) surfaces," Phys. Rev. B **67**, 041308 (2003).
[20]M. Schroeder and D. E. Wolf, "Diffusion on strained surfaces," Surf. Sci. **375**, 129–140 (1997).
[21]L. D. Landau and E. M. Lifshitz, *Theory of Elasticity*, 3rd ed. (Pergamon Press, Oxford, 1986).
[22]C. Wu, V. Y. Zaitsev, and L. V. Zhigilei, "Acoustic enhancement of surface diffusion," J. Phys. Chem. C **117**, 9252–9258 (2013).
[23]A. E. Romanov, P. M. Petroff, and J. S. Speck, "Lateral ordering of quantum dots by periodic subsurface stressors," Appl. Phys. Lett. **74**, 2280–2282 (1999).
[24]Q. Xie, A. Madhukar, P. Chen, and N. P. Kobayashi, "Vertically self-organized InAs quantum box islands on GaAs(100)," Phys. Rev. Lett. **75**, 2542–2545 (1995).
[25]J. Tersoff, C. Teichert, and M. G. Lagally, "Self-organization in growth of quantum dot superlattices," Phys. Rev. Lett. **76**, 1675–1678 (1996).
[26]M. E. Siemens, Q. Li, M. M. Murnane, H. C. Kapteyn, R. Yang, E. H. Anderson, and K. A. Nelson, "High-frequency surface acoustic wave propagation in nanostructures characterized by coherent extreme ultraviolet beams," Appl. Phys. Lett. **94**, 093103 (2009).
[27]M. Schubert, M. Grossmann, O. Ristow, M. Hettich, A. Bruchhausen, E. C. S. Barretto, E. Scheer, V. Gusev, and T. Dekorsy, "Spatial-temporally resolved high-frequency surface acoustic waves on silicon investigated by femtosecond spectroscopy," Appl. Phys. Lett. **101**, 013108 (2012).
[28]D. Nardi, E. Zagato, G. Ferrini, C. Giannetti, and F. Banfi, "Design of a surface acoustic wave mass sensor in the 100 GHz range," Appl. Phys. Lett. **100**, 253106 (2012).